Peer-reviewed version available at *Viruses* **2020**, *12*, 470; doi:10.3390/v12040470

Article

Experimental Infection of Adapted Influenza B Virus in Mice Model

Elena Prokopyeva[1,2*], Olga Kurskaya[1], Ivan Sobolev[1], Mariia Solomatina[1], Tatyana Murashkina[1], Anastasia Suvorova[1], Alexander Alekseev[1], Daria Danilenko[3], Andrey Kommissarov[3], Artem Fadeev[3], Alexander Shestopalov[1], Alexander Dygai[4], Kirill Sharshov[1]

1. Department of Development And Testing of Pharmacological Agents, Federal Research Center of Fundamental and Translational Medicine, Novosibirsk, Russia; e.prokopeva@g.nsu.ru (E.P.); kurskaya_og@mail.ru (O.K.); sobolev_i@hotmail.com (I.S.); Mariaza@ngs.ru (M.S.); murashkinatatiana89@gmail.com (T.M.); asuvorova153@gmail.com (A.S.) al-alexok@ngs.ru (A.A.); shestopalov2@ngs.ru (A.S.); sharshov@yandex.ru (K.S.)
2. Medical Department, Novosibirsk State University, Novosibirsk, Russia; e.prokopeva@g.nsu.ru (E.P.)
3. Department of etiology and epidemiology, Smorodintsev Research Institute of Influenza, Saint Petersburg, Russia; daria.baibus@gmail.com (D.D.); andrey.komissarov@influenza.spb.ru (A.K.); afadeew@gmail.com (A.F.)
4. Goldberg Research Institute of Pharmacology and Regenerative Medicine Clinic, Tomsk, Russia; dygai_am@pharmso.ru (A.D.)

* Correspondence: e.prokopeva@g.nsu.ru

Abstract: Over the years influenza B virus (IBV) contribute annual disease and can lead to serious respiratory disease among humans. More attention should be paid to the mammalian adaptive processes of B viruses and development of vaccines against current influenza. Because of preclinical trials of anti-influenza drugs are conducted mainly on mice, we developed adequate animal model using antigenically-relevant IBV strain for testing anti-influenza drugs and protective efficacy of flu vaccines. We serially passaged Victoria lineage (clade 1A) IBV 17 times in BALB/c mice. The adaptive amino acid substitutions were found in HA (T214I) and NA (D432N). By the electron microscopic examination, we showed spherical and elliptical shapes of IBV. Light microscopy showed that mouse-adapted B virus caused influenza pneumonia on day 6 post inoculation.

We evaluated the illness pathogenicity, viral load and histopathological features of mouse-adapted IBV and estimated anti-influenza drugs and vaccine efficiency *in vitro* and *in vivo*. Assessment of investigational anti-influenza drug *oseltamivir ethoxisuccinate* and flu vaccine Ultrix® revealed effectivity against our mouse-adapted influenza B virus.

Keywords: influenza B virus; mammalian adaptation; amino acid substitutions; pathogenicity; influenza model; animal model; virulence; antiviral drugs

1. Introduction

Influenza B virus (IBV) belongs to the family *Orthomyxoviridae* [1]. They were first isolated in 1940, and since the 1980s two IBV genetic lineages have been identified: B/Victoria/2/87 (B/Vic) and B/Yamagata/16/88 (B/Yam). These lineages differentiated by differences in hemagglutinin (HA) and neuraminidase (NA), which almost have no antigenic crossover in the hemagglutination inhibition assay [2, 3]. Due to the fact that IBV has been isolated from both humans and seals, the reservoir remains unknown [4, 5]. Infection of human caused by IBV can lead to serious respiratory disease, complications of which are particularly common among children of primary school age (5-8 years) [6]. Data for the United States for each epidemic season from 2004-2011 (excluding the 2009 pandemic) show that between 22% and 44% of all childhood influenza-related deaths were caused by IBV infection. More over from 2004 to 2013 Canadian researchers found significantly higher mortality rates due to IBV compared to influenza A virus

in children younger than 16 years of age [7]. In Europe influenza B accounted for 63% of all influenza cases in the 2017-2018 epidemic season [8]. A number of studies using *ex-vivo* (explant) cultures of human bronchus or lung have shown that IBV are capable of causing severe lower respiratory tract infections; these frequently lead to fatal complications [9].

Seasonal influenza vaccines are divided into types: trivalent, which consists of influenza A/H1N1, A/H3N2, and one influenza B strain (B/Yam or B/Vic); or quadrivalent, which contains all four strains. The emerging threat of IBV has been recently recognized [10], and seasonal influenza vaccines are moving towards quadrivalent types [11, 12, 13]. Vaccines designs seek to provide protection against seasonal influenza viruses by eliciting antibody responses to surface viral HA proteins. Constant antigenic drift in HA necessitates regular updating of vaccine strains to ensure that the antigenic profile of circulating strains and vaccine components match [14]. According to the CDC, the effectiveness of quadrivalent vaccine is 28% among the especially susceptible, namely children within the age group of 9–17 years of age [15].

Despite the fact that IBVs has repeatedly caused human epidemics, its genetic determinants of virulence and transmission are still poorly understood. Limited data on the range of hosts and the absence of an animal model complicate several areas: study of pathogenicity factors; IBV modes of transmission; and assessment of antiviral drugs and vaccines effectiveness. The aim of this study was to develop better infection models, using clinically-relevant viruses, which facilitate testing of (anti-influenza) vaccine-induced protection. BALB/c mice were infected with mouse-adapted influenza B virus and were characterized for illness, inflammation, viral load and histopathology; and also, were estimated anti-influenza drugs and vaccine efficiency *in vitro* and *in vivo*.

2. Materials and Methods

All manipulations with animals were approved by the Ethics Committee of the Federal Research Center of Fundamental and Translational Medicine (No. 2017-15).

2.1. Viral adaptation

The virulence of the B virus was increased by serial passages in the lungs of 8-week-old male BALB/c (*n*, 7 per group) mice (State Research Center of Virology and Biotechnology VECTOR (FSRI SRC VB VECTOR), Novosibirsk, Russia). Seven mice were lightly anesthetized with Rometar (20 mg/kg) (Bioveta, Czech Republic) and intranasally infected (i.i.) with 50 µl of phosphate-buffered saline (PBS) containing 10^4 $TCID_{50}$/ml (50% tissue culture infective dose) of the wild type IBV strain B/Novosibirsk/40/2017 (*B/2017*) that were isolated from human in 2017 in Novosibirsk, Russia. Three of seven mice from each passage with the most evident symptoms were sacrificed by decapitation on 3rd day post-infection (d.p.i.). The lungs of these mice were used to prepare 10% homogenates in PBS. Subsequently, new groups of mice were anesthetized with same anaesthetic and i.i. with 50 µl of 10% lung homogenate. In parallel, viral replication of viruses in the lungs of the sacrificed mice was measured by titration of a 10% homogenate using MDCK cell culture [16]. Four of seven mice from each group, at each passage, were monitored daily for 14 d.p.i for signs of illness, weight loss, or lethality. After 17 passages in total were registered the clinical signs: significant reduction in body weight (up to 30%); hypothermia; ruffled fur; mice began to huddled together. The wild type IBV strain *B/2017* and mouse-adapted variant (strain B/Novosibirsk/40/2017-MA (*B/2017-MA*)) were patented [17]. The mouse infectious dose (MID_{50}) of the virus *B/2017-MA* was 4.6±0.26 $\log_{10}TCID_{50}$/ml, or 1.88 $TCID_{50}$.

To evaluate the pathogenicity of *B/2017* and *B/2017-MA* viruses, groups of six 6-week-old male BALB/c mice (*n*, 10 per group) were anesthetized with Rometar (20 mg/kg) and i.i. with 50µL of PBS containing 10^4 $TCID_{50}$/ml and 10 MID_{50}, respectively. Intact mice (*n*, 3 per group) were i.i. with 50 µl of PBS (pH 7.2) and serve as control. Body weight and temperatures changes, and mouse survival rate were monitored daily for 14 d.p.i., and mice that lost more than 25% of their body weight were euthanized. Body weight was measured by using a laboratory animal weighing analytical balances MASSA-K VK-1500 (MASSA-K, Russia), and body surface temperature was taken from the ear canal using a hand-held infrared thermometer «AccuVET» (Mesure technology Co., LTD).

To detect the tissue distribution of *B/2017* and *B/2017-MA* viruses, on days 3 and 6 p.i., three mice were sacrificed and organ samples of lungs, brain, heart, liver, kidneys, spleen harvested in 1 mL of PBS. Then

samples were homogenized and centrifuged, viral titers in the homogenized supernatants were determined by the Kerber method with Ashmarin–Vorobyov modification. To assess by light and electron microscopy pathological lesions from mice infected with of *B/2017* and *B/2017-MA* viruses, their lungs were harvested at 3rd and 6th d.p.i.

2.2. Light microscopic examination

Lungs from 3 animals in each group (`*B/2017* infected` and `*B/2017-MA* infected`) were taken for examination by light microscopy on the 3rd and 6th d.p.i. and subsequently fixed in 4% formalin solution, dehydrated (according to the standard procedure), and embedded into paraffin. Then 4-5 microns thick paraffin sections were obtained using a HM 340E rotary microtome (Carl Zeiss, Germany) and stained by H&E method. Light microscopy and photography were carried out using an Axioskop 40 microscope (Carl Zeiss, Germany).

2.3. Electron microscopic examination

Lung samples were taken on the 3rd and 6th d.p.i. with *B/2017* and *B/2017-MA* viruses. Samples were fixed with 2.5% glutaraldehyde in 0.1 M phosphate buffer pH 7.4 for 4 hours at 4°C; re-fixed with 1% osmium tetroxide in 0.1 M phosphate buffer pH 7.4 at 4 °C for 2 h; then dehydrated in ethanol (50˚, 70˚, 96˚, 100˚) followed by acetone and Araldite-Epon mixture (1:6) (SPI, USA) with the addition of the catalyst DMP-30 and polymerized at 60°C. Semi-thin sections were prepared from solid blocks, stained with Azur II and examined in a light microscope to highlight areas for ultrathin section. Ultrathin sections were cut by EM UC7 ultramicrotome (Leica, Wien, Austria). Sections were stained with uranyl acetate followed by lead citrate (SPI, USA). The samples were examined on a transmission electron microscope LIBRA 120 (Carl Zeiss, Germany) at 100 kV. The images were made by a digital camera Veleta (SIS, Germany).

2.4. Sequencing and GISAID accession numbers

Viral RNA was extracted using QIAamp Viral RNA Mini Kit (QIAGEN) according to the manufacturer's instructions. Whole genome amplification of influenza B genome was performed using SuperScriptTM III One-Step RT-PCR System with PlatinumTM Taq High Fidelity DNA Polymerase (Thermo Fisher Scientific) with modifications [18].

Products of PCR were analyzed by agarose gel electrophoresis, and sequencing was performed using the Illumina MiSeq platform. Paired-end libraries for MiSeq platform were prepared using Nextera XT DNA Library Prep Kit (Illumina). The sequencing library was quantified using NEBNext Library Quant Kit (NEB). Library size was assessed using Agilent Bioanalyzer 2100.

MiSeq v2 reagent kit (300-cycle; 2 × 150-bp PE) (Illumina) was used for sequencing. Nucleotide sequences of *B/2017* and *B/2017-MA* strains are available in the GISAID with the following accession numbers: EPI_ISL_338315 and EPI_ISL_338316, respectively.

2.5. Genetic analysis

The IBV nucleotide sequences being investigated were combined with sequences retrieved from the GISAID database. For multiple alignments, a MUSCLE programme was used [19]. Comparative pairwise sequence alignment of 2 investigated strains was performed via BioEdit. Phylogenetic trees were built via MEGA 5 using Maximum Likelihood, utilizing the general time reversible (GTR) nucleotide substitution model. Bootstrap support values were generated using 500 rapid bootstrap replicates.

2.6. Determination of susceptibility to neuraminidase inhibitors

The susceptibility of *B/2017* and *B/2017-MA* strains to oseltamivir (Hoffmann-La Roche, Basel, Switzerland) were evaluated by published NA inhibition assays [20, 21]. Briefly, viruses were standardized to a NA activity level 10-fold higher than that of the background, as measured by the production of fluorescent product from methylumbelliferyl-N-acetylneuraminic acid (MUNANA) substrate (Sigma-Aldrich, Darmstadt, Germany). Drug susceptibility profiles were determined by the extent of NA

inhibition after incubation with 3-fold serial dilutions of NAIs. The 50% inhibitory concentrations (IC_{50}) were determined from the dose-response curve.

In this study, a new neuraminidase inhibitor (ethyl (3S,4R,5S)-4-acetamido-5-amino-3-(1-ethylpropoxy)cyclohex-1-en-1-carboxylate ethoxy succinate (*oseltamivir etoxisuccinate*) [22] which features antiviral activity was used. The novel compound is prepared by treatment of ethyl(3S,4R,5S)-4-acetamido-5-amino-3-(1-ethylpropoxy)cyclohex-1-en-1-carboxylate with ethoxy succinic acid in ethyl acetate.

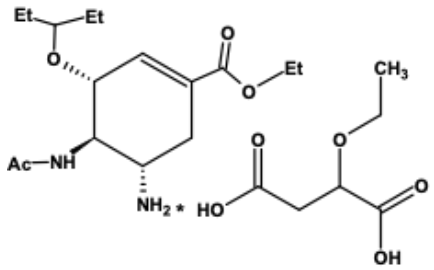

Scheme 1. Ethyl (3S,4R,5S)-4-acetamido-5-amino-3-(1-ethylpropoxy)cyclohex-1-en-1-carboxylate ethoxy succinate.

2.7. Determination of anti-influenza drugs efficacy

We studied anti-influenza efficacy of *oseltamivir etoxisuccinate* and Tamiflu® on 6-8-week-old BALB/c mice (FSRI SRC VB VECTOR) (*n*, 10 per group). All mice of groups №№1-3 were lightly anesthetized with Rometar (2 mg/kg) and then i.i. with 10 MID_{50} of *B/2017-MA* strains in 50 µl. Mice of group №4 were i.i. with 50 µl of PBS and served as control. Then mice of group №1 were treated *per os* by 25 mg/kg/day of *oseltamivir etoxisuccinate* with dose of (200 µl of each) during 5 d.p.i.; mice of group №2 were treated *per os* by same dose with Tamiflu® during 5 d.p.i. Mice from group №3 received 200-µl of distilled water *per os* during 5 d.p.i. All animals were monitored for illness signs, weight loss, temperature changes, mortality, and lethality over 14 d.p.i.

2.8. Mouse Immunization and Inoculation

6–8-week-old male BALB/c mice (FSRI SRC VB VECTOR) were randomly distributed into 3 groups (*n*, 10 per group). Mice were twice (prime boost) immunized subcutaneously (i.s.) with 0,25 µl vaccine Ultrix® (Russia) containing purified surface antigens from influenza strain B/Colorado/06/2017 (lineage B/Victoria/2/87).

On the 14th day after second immunization mice were lightly anesthetized with Rometar (20 mg/kg) (Bioveta, Czech Republic) and i.i. with 50 µl of PBS containing 10^4TCID_{50} of the *B/2017-MA* virus or sterile PBS. At 3rd and 6th d.p.i., 3 animals from each group were humanely euthanized for tissue collection. Lungs were collected for virus titer quantification, light and electron microscopic examinations. At 21 d.p.i., mice were bled from the submandibular vein for serology. Clinical signs of disease such as body weight and temperature changes, mortality and morbidity were monitored daily throughout the study.

2.9. Statistical analyses.

All *in vitro* assays were performed at least twice in triplicate. Virus titers were calculated by the Kerber method with Ashmarin–Vorobyov modification [23], as follows: $\log_{10}TCID_{50}/mL = lgDn - \delta(\Sigma Li - 0.5)$.

For multiple comparisons, two-way analysis of variance (ANOVA) was performed. A *P* value below 0.05 was considered significant.

3. Results

3.1. Viral adaptation

To study the adaptation of B virus isolated from human, we serially passaged the wild type IBV Victoria lineage strain *B/2017* in BALB/c mice. After 17 passages total, mouse-adapted B virus *B/2017-MA* was obtained. We compared the pathogenicity of *B/2017* and *B/2017-MA* strains. Groups of twelve 6-8-

week-old male BALB/c mice were i.i. with 50μL of *B/2017*, or *B/2017-MA* viruses at 10^4TCID$_{50}$ (10 MID$_{50}$). Body weight and temperature changes, morbidity and mortality were monitored during 14 d.p.i, and the PBS-inoculated group of mice served as the control. On the 3rd and 6th d.p.i., 3 animals from each group were sacrificed by decapitation, and internal organs samples (lungs, brain, heart, liver, kidneys, spleen) were taken for comparative virological analysis. On day 3 and 6 p.i., lungs were taken for examination by electron microscopy.

All mice i.i. with *B/2017* virus survived and showed no obvious clinical signs such as body weight and temperature changes (Figure 1A,B). In contrast, in the another experimental group of mice i.i. with *B/2017-MA* were ditected gradually weight loss: approximately 10% at 3 d.p.i., 15% at 4 d.p.i., 20% at 5 d.p.i., 25% at 6 d.p.i., and 30% at 7 d.p.i. (Figure 1A). Temperature measurements indicated the peak infection time frame to be from the 4th to the 7th d.p.i. (Figure 1B).

Figure 1. Comparative analysis of *B/2017* and *B/2017-MA* strains, and assessment of anti-influeza drugs against mouse-adapted influenza B virus *in vivo*

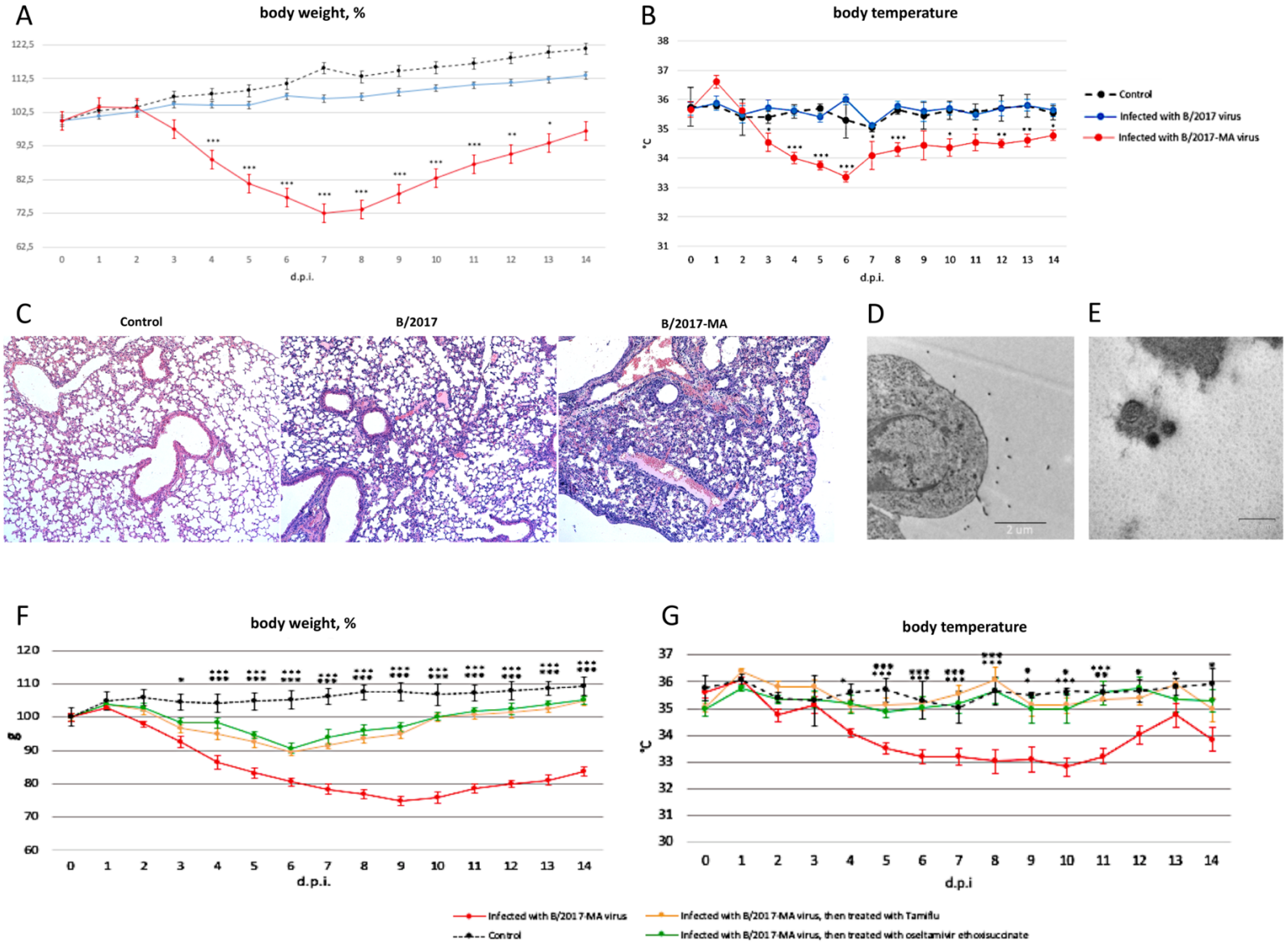

Figure 1. Comparative analysis of *B/2017* and *B/2017-MA* strains, and assessment of anti-influeza drugs against mouse-adapted influenza B virus *in vivo*

Note: A (body weight) and B (body temperature): intact mice received PBS (dotted black line); mice intranasally infected with 10^4 $TCID_{50}$ of B/2017 strain (blue line); mice intranasally infected with 10 MID_{50} of B/2017-MA strain (red line). ✶ , p<0.05;✶ ✶, p < 0.01;✶ ✶ ✶, p < 0.001-reliability when comparing data from groups of infected mice.

C - lungs from mice euthanized 6 days post innoculation were collected and were preserved in 10% formalin for histopathological examination by H&E staining. Images were taken at x40 magnification.

D - budding of influenza B virions from the surface of type 1 alveolar cells on the 3rd day post infection with *B/2017-MA* strain. bar = 20 microns.

E – virions of influenza B; bar = 200 nm.

F (body weight) and G (temperature) of: intact mice received PBS (dotted black line); mice infected intranasally with 10 MID_{50} of B/2017-MA strain (red line); mice infected with 10 MID_{50} of B/2017-MA strain and treated with Tamiflu® (orange line); mice infected with 10 MID_{50} of B/2017-MA strain and treated with *oseltamivir ethoxisuccinate* (green line).✶ , p<0.05;✶ ✶, p < 0.01;✶ ✶ ✶, p < 0.001-reliability when comparing data from groups of infected mice.

At 3 and 6 dpi, three mice were sacrificed and their organs (lungs, brain, heart, liver, kidneys, spleen) were harvested. Viral titers in the collected organs were determined by the Kerber method with Ashmarin–Vorobyov modification. The strain *B/2017* could replicate in mouse lungs only 3 days with titers 2.9±0.2 $log_{10}TCID_{50}$/ml. In contrast, strain *B/2017-MA* replicated very well in mouse lungs, with higher titers and longer period: on 3rd d.p.i. titer was 3.5±0.1 $log_{10}TCID_{50}$/ml, and on 6th d.p.i. - 3.3±0.3 $log_{10}TCID_{50}$/ml. Therefore, the mouse-adapted B virus strain *B/2017-MA* displayed much higher replication capability in mouse lungs.

Histopathological analysis of mice lungs infected with the *B/2017* virus were found out a slight damages such as small number of eosinophilic cells in the bronchioles, small blood filling of the capillaries, and edema with a high protein content on 6th d.p.i. (Figure 1C). In contrast, on the same d.p.i., pathomorphological changes in lungs of mice infected with the *B/2017-MA* virus were more pronounced due to viral triggered apoptosis, leading to desquamation of bronchiol epithelium. Also were seen greater number of eosinophilic cells in the bronchioles, lymphocytic infiltration of lungs various parts, and capillaries stasis (Figure 1C). All of the pathomorphological changes listed were predominantly located in the root, cranioventral and middle regions of the left and right lungs of infected *B/2017-MA* virus mice.

Electron microscopic examination revealed the budding of virions from the surface of type 1 alveolar cells on the 3rd d.p.i. in samples from *B/2017-MA* group mice (Figure 1D,E). Interestingly to note that various virion morphologies were seen: spherical or elliptical, but no filamentous.

3.2. Sequencing and Genetic analysis

According to nucleotide sequences analysis of all eight genome segments, the *B/2017* virus and, consequently, its mouse-adapted variant *B/2017-MA* belong to the B/Vic genetic lineage. In addition, analysis of these strains` HA amino acid sequences revealed mutations (I117D, N129D, V146I) relative to earlier reference strains. These mutations are characteristic of strains belonging to the 1A genetic subgroup of the B/Vic lineage. The strains` NA substitutions were also found feature amino acid substitutions characteristic of genetic group 1A of the B/Vic lineage (N340D, E358K, S295R, I120V, and K220N). To assess the phylogenetic relationships between B/2017 and B/2017-MA, all genome segments were analyzed using phylogenetic dendrograms. Analysis used IBV nucleotide sequences, available in the GISAID database, isolated from residents of Russia and Kazakhstan, as well as vaccine and reference strains according to WHO classification.

According to dendrograms (Suplementary Materials, Figures 1-8), the studied strains form a common phylogenetic group with other isolates from Novosibirsk, as well as strains from the neighbour Altai region and the Republic of Kazakhstan. At the same time, all of them are phylogenetically distanced (although only slightly) from IBV strains isolated in other Russian regions.

To identify strains that are most genetically related to the *B/2017* and *B/2017-MA* strains, BLAST analysis was performed. The results revealed that studied strains are 99-100% identical to the IBV variants that circulated in the human population in the Novosibirsk region, Altai, and Republic of Kazakhstan

(Suplementary Materials, Table 1). Thus, strain *B/2017* is typical genetic variant of the IBV that circulated during 2016-2017 epidemic season, and is the most genetically related to the strains that circulated in Asia at that time.

Comparative analysis of nucleotide and amino acid substitutions between the two strains (*B/2017* vs *B/2017-MA*) showed the presence of synonymous (not leading to amino acid substitution) nucleotide substitution in the PB1 segment - A2175G. Additionaly, nucleotide substitution in the HA segment (C641T) led to the amino acid substitution in the HA protein (T214I). According to the Flusurver resource [24], the detected substitution is rare and present in 0.46% HA of IBVs isolated from 2008 to 2016. The identified amino acid substitution is localized in the antigenically active subunit HA-HA1, which can potentially affect the biological properties of the virus. In the sequence encoding , a nucleotide substitution (G1294A), which leads to the amino acid change D432N, was detected. According to the Flusurver resource [24], this substitution has only been found in one strain (B/Hawaii/37/2017) so far.

3.3. Assessment of Antiviral Drug Therapy In Vitro and In Vivo

In our work we estimate the IC_{50} of *oseltamivir ethoxisuccinate* that necessary to reduce NA activity of *B/2017* and *B/2017-MA* strains and it were 75.68±10.42 μM and 107.645±53.96 μM, respectivly. The IC_{50} of Tamiflu® that necessary to reduce NA activity of strain *B/2017* was 122.7±24.04 μM, and for strain *B/2017-MA* was 43.47±8.12 μM. Thus, analyzes of the NA inhibition *in vitro* were showed that *oseltamivir ethoxisuccinate* and Tamiflu® reduced the neurominidase activity of *B/2017* and *B/2017-MA* strains equally effectively.

Also in our study were performed anti-influenza drugs efficiency *in vivo*, which showed no significant body wight and temperature changes between groups of animals i.i. with *B/2017-MA* strain and then treated *per os* during 5 days with *oseltamivir ethoxisuccinate* or Tamiflu® (Figure 1F,G). All treated with anti-influenza drugs mice lost no more than 10% of body weight and began to recovere from the 7th d.p.i. Also no hipothermia were detected among them. Therefore, was shown that innovative drug (*oseltamivir ethoxisuccinate*) revealed high effectiveness against the mouse-adapted B virus similarly Tamiflu®.

3.4. Assessment of Vaccine Efficiency Against Mouse-adapted Influenza B Virus In Vivo

We performed assessment of vaccine efficiency against mouse-adapted *B/2017-MA* strain *in vivo*. Previously BALB/c mice were immunized with purified surface antigens from influenza strain B/Colorado/06/2017 (lineage B/Victoria/2/87) (Ultrix®, Russia) in 0,25 μl twice (prime boost), and on 21 day after vaccination mice were i.i. with *B/2017-MA* strain. Non-immunized and infected mice served as control group.

Infection induced by *B/2017-MA* strain in non-immunized mice was characterized by body weight lost and hypothermia from the 2nd d.p.i, and conjunctivitis (up to 30%), with onsets between days 1 to 3 d.p.i. (Figure 2A,B,C). All mice of this group huddled together, and their fur was ruffled on the 4th d.p.i. Peak illness was determined to be from 5th up to 10th d.p.i., as seen by a large percent of total body weight lost and visibly increased breathing effort caused by severe pathological processes in the lungs (Figure 2D). Some of mice necessitated humane culling on the 9th (n=2) and the 10th d.p.i. (n=2). All unimmunized and i.i. with *B/2017-MA* strain mice lost significant amounts of body weight relative to the comparison groups ($P, < 0.001$). In addition, mice `vaccinated and *B/2017-MA* infected` experienced statistically-significant reductions in body weight from the 4th up to 7th d.p.i., compared to the control group ($P, < 0.001$). Temperatures were also measured, and statistically-significant differences ($P, < 0.001$) between the `vaccinated and *B/2017-MA* infected` and intact mice were detected at 5th, 7th and 10th d.p.i. The data suggest that the adapted IBV virus affects vaccinated mice for up to 10 d.p.i. No other influenza signs were observed in vaccinated mice, which indicates mild IBV illness and effective Ultrix® vaccination.

Preprints (www.preprints.org) | NOT PEER-REVIEWED | Posted: 3 February 2020 doi:10.20944/preprints202002.0022.v1

Peer-reviewed version available at Viruses 2020, 12, 470; doi:10.3390/v12040470

Figure 2. Assessment of vaccine efficiency against mouse-adapted influenza B virus *in vivo* and *in vitro*

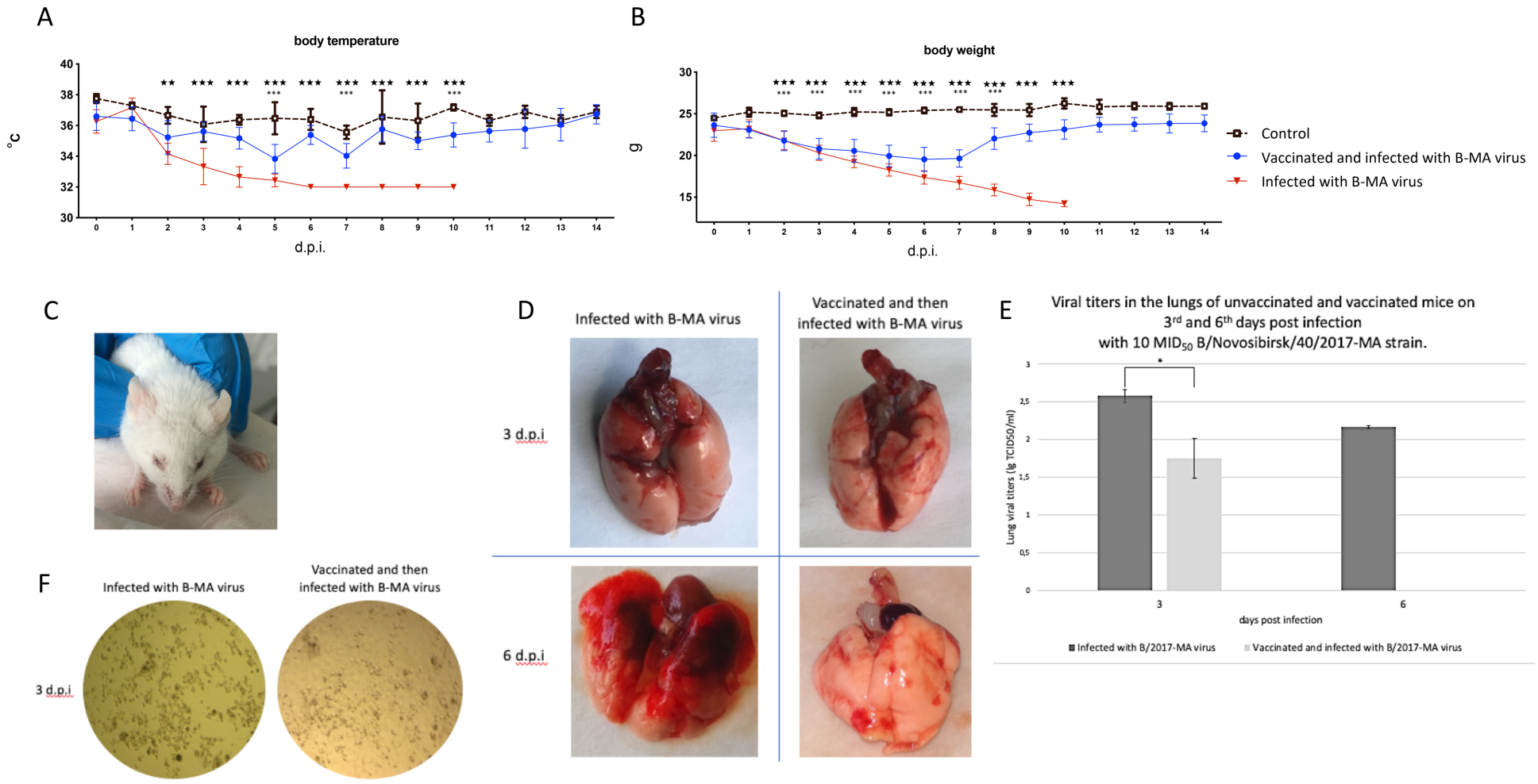

Figure 2. Assessment of vaccine efficiency against mouse-adapted influenza B virus *in vivo* and *in vitro*

Note: A (body temperature) and B (body weight) of: intact mice received PBS (dotted black line); vaccinated and infected intranasally with 10 MID_{50} of B/2017-MA strain mice (dark blue line); infected intranasally with 10 MID_{50} of B/2017-MA strain mice (red line); ✶ , $p<0.05$;✶ ✶, $p < 0.01$;✶ ✶ ✶, $p < 0.001$-reliability when comparing data from groups of infected mice.

C - on day 3 day, conjunctivitis in a mouse infected with 10 MID_{50} of B/2017-MA *strain.*

D – lungs of unvaccinated and vaccinated mice on 3rd and 6th days post infection with 10 MID_{50} of *B/2017-MA* strain.

E – viral titers in the lungs of unvaccinated and vaccinated mice on 3rd and 6th days post infection with 10 MID_{50} of *B/2017-MA* strain.

F – cytopathic effect of MDCK cell culture on 3rd day post infection of unvaccinated and vaccinated mice with 10 MID_{50} of *B/2017-MA* strain.

Lung viral loads were assessed *via* MDCK cell culture (all groups) (Figures 2E,F). Virus was detected in lungs *via* $TCID_{50}$ assay on day 3 for all infected mice (Figure 2F). On day 6, virus was only detected in unvaccinated mice (Figure 2F). In the group `vaccinated and *B/2017-MA*`, it was noted that only 10-20% of cells in the walls are affected, but in group of comparison were detected 100% of cytopathic effect (Figure 2F).

Macroscopic examination of unvaccinated mouse lungs revealed inflammation in root and cranioventral regions on the 3rd d.p.i. By contrast, in the group `vaccinated and *B/2017-MA* infected`, minor patchy areas of alveolar hemorrhage (Figure 2D) were seen. By the 6th d.p.i., the inflammatory process had worsened only in lungs of unvaccinated mice, as characterized by interstitial pneumonia, which affected almost lungs, except the caudal sections (Figure 2D). There were no significant differences in lung inflammation on day 6 after challenge in vaccinated mice (Figure 2D).

4. Discussion

Influenza B viruses have real epidemiological significance, especially among children. Together, IBV and influenza A cause significant seasonal burdens. A lack of information about IBV's host range and the need for an adequate animal model have complicated several areas: study of pathogenicity factors and transmission methods; evaluate the antiviral drugs effect, and assessment of vaccine effectiveness. In the field of Virology, there is an entire branch devoted to obtaining recombinant strains for vaccines. Such IBV strains, however, are attenuated and apathogenic for experimental animals. Consequently, they do not provide an opportunity to study the pathological process of influenza infection, which makes it difficult to perform studies of anti-influenza drug effectiveness *in vivo*. Moreover, many of presented recombinant strains have lost their antigenic relevance today.

Because preclinical trials of anti-influenza drugs are conducted mainly on mice [25], we also sought a mouse model. An antigenically-relevant IBV (strain *B/2017-MA*) was developed, used for experimental infection in mice, and the model applied to evaluate the therapeutic and preventive effectiveness of antiviral drugs and vaccines *in vivo* and *in vitro*. Amino acid substitutions associated with IBV adaptation to mice were identified, and, probably, due to them the pathogenicity increased and enhanced replication ability in infected mammals.

On the 6th d.p.i in BALB/c mice, influenza pneumonia featuring leukocyte and lymphocyte infiltration of bronchioles was detected in the lungs of animals infected with mouse-adapted IBV (strain *B/2017-MA*). On the same day, no viral loads were detected in the lung of mice infected with wild type IBV (strain *B/2017*). Despite this fact, pathomorphological changes were registered and characterized as mild disease.

Because the knowledge of the virions structure of influenza B remains limited [26, 27] we used the electron microscopic method. We showed two shapes of virions that are not only spherical, but also elliptical. Perhaps, it is also mean that influenza B virions can have pleomorphick morphological structure.

Comparative analysis of nucleotide and amino acid substitutions between wild strain *B/2017* and it's mouse-adapted variant *B/2017-MA* strain revealed non-synonymous nucleotide substitutions that lead to amino acid substitutions in two proteins, HA and NA. One of the amino acid substitution identified (T214I in HA) localized in the antigenically active subunit HA-HA1, thereby affecting the biological properties of the virus. Interestingly to note that same substitution was present in 0.46% of IBVs reported from 2008 to 2016 [24]. Probably, this fact may explain severe cases and poor clinical outcomes in patients infected with IBV. Another substitution was found in NA and caracterized as rare [24]. In view of the above, we assume that Asn amino acid at position 432 of the NA protein can lead to antiviral resistance and in complex with other substitution in the surface glycoprotein HA might jointly be responsible for the high pathogenicity.

Due to their roles in elevating seasonal morbidity and mortality among humans worldwide, influenza A and B viruses have epidemiological, social, and economic significance [2, 13]. Selective inhibition of neuraminidase is used in the treatment of influenza to control the processes of budding and release of mature virions from the surface of an infected host cell (as a result of cleavage of sialic acid residues from hemagglutinin). In addition, NA plays a key role in the initial stages of infection, ensuring the penetration of influenza viruses into cells. Due to the specific activity of NA, inhibitors work effectively against influenza A and B viruses. Of the two NA inhibitors, oseltamivir phosphate (Tamiflu®) is considered the most effective because of its higher bioavailability (30-100%) compared to Relenza® [21]. However, the use of anti-influenza drugs to prevent and treat diseases is complicated by viral resistance which has been observed in recent years [2, 29]. In addition, it has been shown that Tamiflu® a lot less effective in treating influenza B compared to influenza A [30]. Here, we show that innovative drug *oseltamivir ethoxisuccinate* is the promising drug in the case of strain resistance to Tamiflu. The investigational drug (oseltamivir ethoxisuccinate) is a modified version of Tamiflu, and it displays (like Tamiflu) relatively high effectiveness against the mouse-adapted IBV. Due to the fact that investigational drug (*oseltamivir ethoxisuccinate*) is a modified version of Tamiflu®, and its revealed high effectiveness against the mouse-adapted IBV similarly Tamiflu®, the *oseltamivir ethoxisuccinate* is the promising drug when dealing with resistant strains to Tamiflu®.

More attention should be paid to mammalian adaptation of IBVs and how such procedures and mechanisms can enhance the development of vaccines against current influenza strains. Due to the fact that no significant lung damage was detected in vaccinated mice at day 6 after challenge, we can conclude that Ultrix® quadrivalent vaccine is effective against our mouse-adapted IBV.

5. Conclusions

In this work, we serially passaged a Victoria lineage IBV 17 times in BALB/c mice. The mouse-adapted IBV caused influenza pneumonia on day 6 post inoculation. Apparently, selective accumulation of amino acid substitutions in the mouse-adapted IBV, including changes to HA (T214I) and NA (D432N), may increase pathogenicity following the adaptation and be important for the virions attach to hosts airways; however, the specific effects of these amino acid substitutions on mammalian pathogenicity requires further study. Also, were shown spherical and elliptical shapes virions of IBV.

Assessment of investigational anti-influenza drug *oseltamivir ethoxisuccinate* and flu vaccine Ultrix® revealed effectivity against our mouse-adapted influenza B virus. In summary, we developed adequate animal model by using antigenically-relevant mouse-adapted *B/2017-MA* strain for testing anti-influenza drugs and protective efficacy of flu vaccines *in vitro* and *in vivo*.

Supplementary Materials: The supplementary files cans be found online.

Author Contributions: Conceptualization, E.P. and O.K.; data curation, E.P., O.K., I.S., M.S., T.M., A.S., A.C., A.F., and K.S.; formal analysis, E.P., O.K., I.S., and K.S.; funding acquisition, E.P. and K.S.; investigation, E.P., O.K., I.S., and K.S.; methodology, E.P., O.K., I.S., M.S., T.M., A.S., A.C., and A.F.; project administration, E.P., A.A., D.D., A.S., A.D. and K.S.; resources, E.P., O.K..; software, I.S., A.K., and A.F.; supervision, E.P.; validation, O.K., I.S., A.C., A.F and K.S.; visualization, E.P., M.S.; writing—original draft, E.P., O.K., I.S, and K.S.; writing—review and editing, E.P., O.K., I.S, D.D, A.K., A.F., and K.S.

Funding: This work was funded by the President's grant (agreement # 075-15-2019-1083 (MK-3318.2019.4)) (such part of work as virological and microscopic analyses). Additional funding was provided by the support of the Russian

Scientific Foundation (project # 19-74-10055) (such part of work as sequencing, phylogenetic analysis and determination of susceptibility to neuraminidase inhibitors).

Acknowledgments: We thank Sysolyatin Sergey at the Institute for Problems of Chemical and Energetic Technologies, Biysk, Russia, for providing antiviral drug *oseltamivir ethoxysuccinate.*

Construction of the tree was done using sequences deposited in GISAID. We are grateful to GISAID's EpiFluTM Database (http://www.gisaid.org) and to the authors who provided sequence information.

Conflicts of Interest: The authors declare no conflicts of interest.

References:

1. ICTV. International Committee on Taxonomy of Viruses, 2019, http://www. Ictvonline.org/virusTaxonomy.asp
2. Su, S.; Chaves, S.S.; Perez, A.; et al. Comparing clinical characteristics between hospitalized adults with laboratory-confirmed influenza A and B virus infection. Clin. Infect. Dis. 2014, 59(2), 252-255.
3. McCullers, J.A.; Hoffmann, E.; Huber, V.C.; et al. A single amino acid change in the C-terminal domain of the matrix protein M1 of influenza B virus confers mouse adaptation and virulence. Virology 2005, 336(2), 318–326.
4. Bodewes, R.; Morick, D.; de Mutsert, G.; et al. Recurring influenza B virus infections in seals. Emerging infectious diseases 2013, 19(3), 511-512.
5. Osterhaus, A.D.; Rimmelzwaan, G.F.; Martina, B.E.; et al. Influenza B virus in seals. Science, 2000, 288(5468), 1051-1053.
6. US Department of Health and Human Services. Centers for Disease Control and Prevention. Influenza-associated pediatric deaths — United States, September 2010–August 2011. MMWR Morb. Mortal. Wkly. Rep. 2011, 60, 1233–1238.
7. Tran, D.; Vaudry, W.; Moore, D.; et al. Hospitalization for influenza A versus B. Pediatrics, 2016, 138, e20154643.
8. Adlhoch, C.; Snacken, R.; Melidou, A.; et al. The European Influenza Surveillance Network. Dominant influenza A(H3N2) and B/Yamagata virus circulation in EU/EEA, 2016/17 and 2017/18 seasons, respectively. Euro Surveill. 2018, 23, 13.
9. Bui, C.H.T., Cheung, M.C.; et al. Tropism of influenza B viruses in human respiratory tract explants and airway organoids. Eur. Respir. J. 2019; in press [https://doi.org/10.1183/13993003.00008-2019].
10. Sharma, L.; Rebaza, A.; Dela Cruz, C.S. When "B" becomes "A": the emerging threat of influenza B virus. Eur. Respir. J. 2019, 54, 1901325 [https://doi.org/10.1183/13993003.01325-2019].
11. CDC. Influenza Vaccination: A Summary for Clinicians. https://www.cdc.gov/flu/professionals/ vaccination/ vax-summary.htm
12. WHO. Recommended composition of influenza virus vaccines for use in the 2017-2018 northern hemisphere influenza season https://www.who.int/influenza/vaccines/virus/recommendations/201703_recommendation. pdf
13. Shaw, M.W.; Xu, X.; Li, Y.; et al. Reappearance and global spread of variants of influenza B/Victoria/2/87 lineage viruses in the 2000-2001 and 2001-2002 seasons. Virology, 2002, 303(1), 1-8.
14. McCullers, J.A. Insights into the interaction between influenza virus and pneumococcus. Clinical microbiology reviews, 2006, 19(3), 571–582.
15. US Department of Health and Human Services. Centers for Disease Control and Prevention. Seasonal Influenza Vaccine Effectiveness, 2017–2018. www.cdc.gov/flu/vaccines-work/2017-2018.html?CDC_AA_ refVal=https%3A%2F%2Fwww.cdc.gov%2Fflu%2Fprofessionals%2Fvaccination%2Feffectiveness-year%2F 2017 -2018.html Date last updated: February 25, 2019. Date last accessed: June 20, 2019.
16. Manual for the laboratory diagnosis and virological surveillance of influenza. WHO Global Influenza Surveillance Network, 2011, 153.
17. Prokopyeva, E. A.; Kurskaya, O. G.; Sobolev, I. A.; Sharshov, K. A.; Murashkina, T. A.; Derko, A. A.; Alekseev, A. Yu.; Shestopalov, A.M.; Sysolyatin, S.V.; Vorozhtsov, A.B.; Vaizova, O.E.; Sherstoboev, E.Yu.; Dygay, A.M.

Patent № 2703024 "Strain of influenza virus B/Novosibirsk/40/2017-MA for study of therapeutic and preventive efficacy of antiviral drugs in vitro and in vivo". Application № 2019107486. Priority of the invention of March 15, 2019.

18. Zhou, B.; Lin, X.; Wang, W.; Halpin, R.A.; Bera, J.; Stockwell, T.B.; Barr, I.G.; Wentworth, D.E. Universal Influenza B Virus Genomic Amplification Facilitates Sequencing, Diagnostics, and Reverse Genetics. J. Clin. Microbiol., 2014, 52(5), 1330–1337.
19. Edgar, R.C. MUSCLE: multiple sequence alignment with high accuracy and high throughput. Nucleic Acids Res. 2004;32(5):1792–1797.
20. Gubareva, L.V.; Webster, R.G.; Hayden, F.G. Detection of influenza virus resistance to neuraminidase inhibitors by an enzyme inhibition assay. Antiviral. Res., 2002, 53(1), 47–61.
21. Potier, M, Mameli L, Bélisle M, Dallaire L, Melançon SB. Fluorometric assay of neuraminidase with a sodium (4-methylumbelliferyl-alpha-D-N-acetylneuraminate) substrate. Anal Biochem. 1979; 94(2):287–296.
22. Dygay, A.M.; Zhdanov, V. V.; Sysolyatin, S. V.; Kalashnikov, A. I.; Vorozhtsov, A. B.; Sherstoboev, E. Yu.; Zhukov, A. S.; Vaizova, O. E.; Prokopyeva, E.A. Patent № 2639158 "Ethyl (3s,4r,5s)-4-acetamido-5-amino-3-(1-ethyl propoxy) cyclohex-1-en-1-carboxylate etoxy succinate as anti-viral drug and method for its production". Application № 2016126652. Priority of the invention of 01 July 2016.
23. Ashmarin, A. Vorobyov. Statisticheskie metody v mikrobiologicheskich issledovanijach. Medgiz, Leningrad; Russian 1962, 180.
24. Flusurver. Real-time surveillance of influenza mutations. https://flusurver.bii.a-star.edu.sg
25. Guidance for Industry Influenza: Developing Drugs for Treatment and/or Prophylaxis. http://www.fda.gov/Drugs/GuidanceComplianceRegulatoryInformation/Guidances/default.htm
26. Noda, T.; Native Morphology of Influenza Virions. Front Microbiol. 2011; 2: 269.
27. Maeno, K.; Replication of influenza B viruses: biological functions of viran neuraminidase. Nagoya J. Med. Sci. 1994, 57, 1 – 17.
28. WHO. (2018). http://www.euro.who.int/ru/health-topics/communicable-diseases/influenza/seasonal-influenza/clinical-management/about-antiviral-drugs
29. Burceva, E. Review of efficacy data and monitoring of oseltamivir susceptibility to influenza virus strains. Vrach = Doctor (In Russ.), 2010, 12, 67-70.
30. Sato, M.; Saito, R.; Sato, I.; et al. Effectiveness of oseltamivir treatment among children with influenza A or B virus infections during four successive winters in Niigata City, Japan. Tohoku J. Exp. Med. 2008, 214, 113–120.